NONPARAMETRIC CLASSIFIER OF BURIED MINES USING MWIR IMAGES

Bo Ling*[a], Anh H. Trang[b], Chung Phan[b]
[a]Migma Systems, Inc., 1600 Providence Highway, Walpole, MA 02081
[b]US Army RDECOM CERDEC NVESD, Fort Belvoir, VA 22060

ABSTRACT

Under Army SBIR Phase I funding, we have developed a nonparametric buried mine classifier using MWIR images. We start with our new image segmentation method based on the wavelet transform. Instead of thresholding the original MWIR images, we first apply the wavelet transform to MWIR image and estimate a threshold value in the corresponding wavelet domain. The small wavelet coefficients are associated with the noise and background clutters appeared in the original image. We then map this threshold in the wavelet domain back to MWIR image domain by applying the inverse wavelet transform. This new threshold is subsequently used to segment the MWIR images and extract small image chips (patches) containing potential buried mines for further detection and classification. In order to perform the statistical classification, we have applied Kolmogorov-Smirnov (KS) test, a powerful nonparametric statistical hypothesis test procedure. One major advantage of using KS test for buried mine detection is that we don't need to make any assumptions of the underlying statistical distributions associated with the cluster intensity variation profiles.

Keywords: buried mine detection; Kolmogorov-Smirnov test; cluster intensity variation; statistical hypothesis test

1. INTRODUCTION

Traditional landmine detection techniques are both dangerous and time consuming. Landmines can be square, round, cylindrical, or bar shaped. The casing can be metal, plastic, or wood. These characteristics make landmine detection difficult. The fundamental challenges of buried mine detection arises from the fact that the mean spectral signatures of the disturbed soil areas that indicate mine presence are nearly always very similar to the signatures of mixed background pixels that naturally occur in heterogeneous scenes composed of various types of soil and vegetation. They tend to closely mimic spectral mixtures of the dominant soil and vegetation constituents that exist in the background.

Thermal techniques can be used to detect buried mines that have been buried in the ground for a long time. Most buried mines, to be effective, have to be buried close to the surface. They often have different thermal properties, such as conductivity and mass, from the soil, and thus detection of the buried mine itself does not rely on the properties of the surface soils. Almost all soils have spectral structures due to the spectral properties of minerals which compose them. Studies have shown that particle size has a very strong effect on spectral properties of the minerals which compose the surface dirt. Thus, even for soil where there is no mineral compositional distinction between the top layer and the subsoil, the differential sorting of sizes will result in different spectral signature.

Behboodian et al. [4] presented a system that uses elastic surface waves and electromagnetic waves for the detection of buried landmines. It mainly uses the acoustic waves to detect the buried landmines. The depth information can be inferred from the Fourier transformed data based on the property that the penetration depth is proportional to the temporal frequency. Mine detection using infrared techniques is primarily based on exploiting temperature differences between pixels on the mines and background pixels [5]. The use of spatial information (e.g., size, shape, and pattern) can provide additional discrimination power, particularly if the mines are resolved into multiple pixels by a high-resolution imaging sensor.

In infrared-based landmine detection applications, the thermal signature is often embedded in noise caused by fluctuations in the soil structure and the surface. To design a detector, Svensson and Lundberg [12] modeled the characteristics of the noise. Difficulties arise when designing a detector as the infrared signatures of buried landmines vary significantly depending on external parameters such as weather, soil moisture, solar radiation, burial depth, and time of burial. To solve these problems, Svensson and Lundberg [13] modeled both the shape and amplitude of the mine signature as outcomes of the stochastic variables respectively, with known prior distributions. The Bayesian Likelihood Ratio Test is used in the classification design. Lundberg [10] proposed to model the set of possible infrared signatures as a scaling with the parameter of the convolution between the top-view shape of the buried object and a smoothing kernel

* bling@migmasys.com; phone 1 508 660-0328; www.migmasys.com

Report Documentation Page

Form Approved
OMB No. 0704-0188

1. REPORT DATE	2. REPORT TYPE	3. DATES COVERED
01 NOV 2006	**N/A**	**-**

4. TITLE AND SUBTITLE	5a. CONTRACT NUMBER
Nonparametric Classifier Of Buried Mines Using Mwir Images	5b. GRANT NUMBER
	5c. PROGRAM ELEMENT NUMBER
6. AUTHOR(S)	5d. PROJECT NUMBER
	5e. TASK NUMBER
	5f. WORK UNIT NUMBER
7. PERFORMING ORGANIZATION NAME(S) AND ADDRESS(ES) **Migma Systems, Inc., 1600 Providence Highway, Walpole, MA 02081**	8. PERFORMING ORGANIZATION REPORT NUMBER
9. SPONSORING/MONITORING AGENCY NAME(S) AND ADDRESS(ES)	10. SPONSOR/MONITOR'S ACRONYM(S)
	11. SPONSOR/MONITOR'S REPORT NUMBER(S)

12. DISTRIBUTION/AVAILABILITY STATEMENT
Approved for public release, distribution unlimited

13. SUPPLEMENTARY NOTES
See also ADM002075., The original document contains color images.

14. ABSTRACT

15. SUBJECT TERMS

16. SECURITY CLASSIFICATION OF:			17. LIMITATION OF ABSTRACT	18. NUMBER OF PAGES	19a. NAME OF RESPONSIBLE PERSON
a. REPORT	b. ABSTRACT	c. THIS PAGE			
unclassified	**unclassified**	**unclassified**	**UU**	**8**	

Standard Form 298 (Rev. 8-98)
Prescribed by ANSI Std Z39-18

depending on a smoothing parameter. The background noise is modeled by means of a quarter-plane causal auto regressive (AR) process. Likelihood ratio test was used in the detection of mines.

Beaven et al. [3] used an abnormal detector to remove the background clutter. Then, they apply spatial cluster and size filtering to the raw filtered output to produce the object detection in both of the filtered image data sets. Joint Multisensor Exploitation is used for fusing registered multiple detector outputs, which makes the decision based on the joint distribution formed by the multiple detector outputs. Filippidis et al. [9] reported an automatic detection using knowledge-based techniques. The fuzzy rule-based fusion is used to combine complementary information derived from sensors to produce an output image showing the likelihood of mine locations. The inputs to the fusion process are the output classification results from ART2 and the MLP (MultiLayer Perceptron), together with the output of the processed IR polarization image. A GA (Generic Algorithm) tool is used to find the optimum structure and inputs of the MLP neural networks.

An important consequence of the marginal spectral separation between buried mine targets and mixed backgrounds is that the conventional projection-based methods of spectral detection, such as matched filtering, statistical anomaly detection, and linear unmixing, cannot provide reliable detection performance [5]. This is because the mine pixels are so spectrally similar to linear mixtures of the prominent background constitutes that any potential mine discriminants must largely function in the spectral subspace defined by the background itself. An algorithm for automatically recognizing mine pixels must therefore be based *not* on global linear projections that suppress the background, but on a local analysis of pixel fluctuations in the background-dominated spectral coordinates. A buried mine detector should search the scene for small patches of contiguous pixels that exhibit relatively low spectral fluctuation and have a mean spectral color which is sufficiently different from the dominant background constituents.

A passive multispectral scanner can be used to detect spectral intensity differences between mines and man-made and natural clutter. The reason for using multispectral analysis is that it has the potential to discriminate between landmines and all other surface clutter. Filippidis et al. [9] trained a neural network classifier to discriminate against clutter and automatically detect landmines. In the study conducted by Batman and Goutsias [3], an unsupervised iterative scheme was used for landmine detection in heavily cluttered scenes. This scheme is based on iterating hybrid multispectral filters that consist of a decorrelating linear transform coupled with a nonlinear morphological detector. It effectively addresses several weaknesses associated with previous adaptations of morphological approaches to landmine detection.

Under Army SBIR Phase I funding, we have developed a nonparametric buried mine classifier using MWIR images. We start with our image segmentation method based on the wavelet transform. Instead of thresholding the original MWIR images, we first apply the wavelet transform to the MWIR image and estimate a threshold value in the corresponding wavelet domain. The small wavelet coefficients are associated with the noise and background clutters appeared in the original image. We then map this threshold in the wavelet domain back to MWIR image domain by applying the inverse wavelet transform. This new threshold is subsequently used to segment the MWIR images and extract small image chips (patches) containing potential buried mines for further detection and classification.

In order to perform the statistical classification, we have applied Kolmogorov-Smirnov (KS) test, a powerful nonparametric statistical hypothesis test procedure. KS-test essentially determines whether or not two data sets are drawn from the same statistical distribution. The null hypothesis is that they have the same distribution. Based on our classifier, a buried mine is detected if the null hypothesis is rejected. Otherwise, the image chip does not contain any buried mines, only background clutters. One major advantage of using KS-test for buried mine detection is that we don't need to make any assumptions of the underlying statistical distributions associated with the cluster intensity variation profiles.

Since the chip size is often too large (e.g., 50×50 pixels) to process in near real time, we apply a 3D unsupervised clustering method, *Adaptive Self-Organizing Maps* (ASOM), to extract the representative pixels from this target chip. Compared to the traditional clustering methods, our ASOM does not need any prior knowledge of the cluster numbers. By self-learning, it finds the optimal number of clusters from the pixels of the image chip. Being able to estimate the number of clusters in an unknown image chip is significant since it is often impossible to have the knowledge of image chip content *a priori*. Unsupervised clustering method such as our 3D ASOM is essential in dealing with real world data processing, including the buried mines detection.

For the representative pixels (i.e., cluster centers) extracted by our 3D ASOM, we scan this clustered chip row-by-row (horizontal scanning) to construct a cluster intensity variation profile. This is accomplished by comparing the pixel intensity values at adjacent cluster centers. Since each cluster center represents all pixels in its cluster, this cluster variation profile essentially captures the significant thermal variation in each image

chip. In our Phase I study, we have found that the cluster intensity variation profiles associated with buried mines are quite different from those constructed from the background clutters. Therefore, we have used this cluster variation profile as our buried mine signature.

Since the thermal variations are dependent on the time of day, different buried mine profiles must be constructed. To detect the buried mines, we have constructed a library of buried mine signatures using the cluster variation profiles for daytime and night time. To detect the buried mines from a given MWIR image, we construct the actual cluster variation profile from this image. Our buried mine classifier is developed to statistically compare this actual profile with all signature profiles in the library. If there is a significant deviation between this actual profile and signatures, the image chip is declared to contain a buried mine, thus, detecting the buried mine. The key to this technology is to determine how to statistically compare the profiles which alawys vary in length.

This paper is organized as follows: The wavelet-based MWIR image thresholding method is given in Section 2. Our cluster trending based buried mine classifier is given in Section 3. The test results using both daytime and night time MWIR images are given in Section 4.

2. WAVELET-BASED MWIR IMAGE THRESHOLDING

Suppose $\mathbf{Y} = [Y_1, Y_2, \ldots, Y_{MN}]^T$ is a vector of pixel values of an image of size $M \times N$. The problem of image thresholding is to find a threshold λ_{image} such that

$$\hat{Y}_i = \begin{cases} Y_i & \text{if } Y_i \geq \lambda_{image} \\ T & \text{if } Y_i < \lambda_{image} \end{cases} \tag{2-1}$$

where T is the smallest pixel value in a given image. The resulting image, $\hat{\mathbf{Y}} = [\hat{Y}_1, \hat{Y}_2, \ldots, \hat{Y}_{MN}]^T$, is significantly compressed (i.e., most clutters are removed) if λ_{image} is properly estimated and larger than most of clutter pixel values. The key is how to estimate this thresholding level, λ_{image}.

Let X be an $M \times N$ image. Basic wavelet thresholding is performed by taking the wavelet transform of the image X, and then estimating the appropriate threshold based on the image content. The thresholding value in the wavelet domain can be expressed in terms of the product of σ_{w} and λ_{w}:

$$\lambda_{\text{wavelet}} = \sigma_{\text{w}} \times \lambda_{\text{w}} \tag{2-2}$$

where both σ_{w} and λ_{w} can be estimated based on the image content.

To estimate λ_{image}, we use the Inverse Discrete Wavelet Transform (IDWT) to map λ_{wavelet} estimated in the wavelet domain to the image domain. A 2D discrete wavelet transform performs three decompositions along horizontal (H), vertical (V) and diagonal (Λ) directions with different threshold levels denoted as t_h, t_v, and t_d, respectively. Denote DH_{t_h}, DV_{t_v}, and $D\Lambda_{t_d}$ as the denoising operators at corresponding threshold levels. We have used the following inverse transform:

$$\hat{X} = W^{-1}\left(DH_{t_h}(W(X)),\, DV_{t_v}(W(X)),\, D\Lambda_{t_d}(W(X))\right) \tag{2-3}$$

and $\hat{\lambda}_{image}$ is extracted from the resulted image.

Figure 1 shows an example where the original MWIR image is given in the left figure and the thresholded image is given in the right. The MWIR image contains both surface and buried mines together with fiducials (ground markers) and background clutters. It can be observed that our wavelet-based image thresholding method has successfully retained both surface and buried mines.

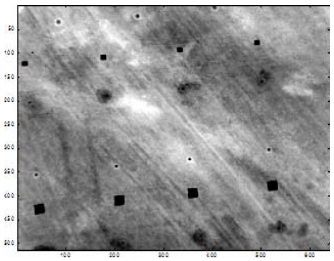

(a) Original MWIR image.

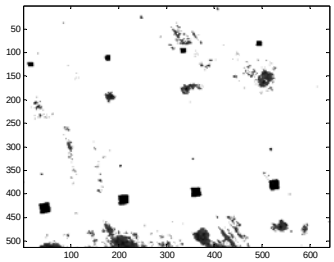

(b) Thresholded image.

Figure 1: An example of our wavelet-based image thresholding method.

To locate the buried mines in the thresholded image, we apply our ASOM (Adaptive Self-Organizing Maps) which is essentially a new data clustering method. However, compared with other existing clustering algorithms, our method does not require any *a prior* knowledge of the number of clusters in the data. It does the clustering by

self-learning and self-teaching. Our 3D ASOM has been applied to the thresholded image to locate potential mines. The center of each cluster indicates the location of a potential mine. Figure 2 shows an example of ASOM applied to the thresholded image. The clusters (small circles) and their centers have been plotted on the original MWIR image.

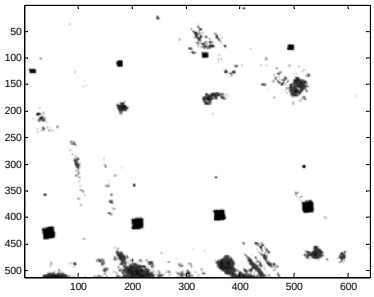

(a) Thresholded image.

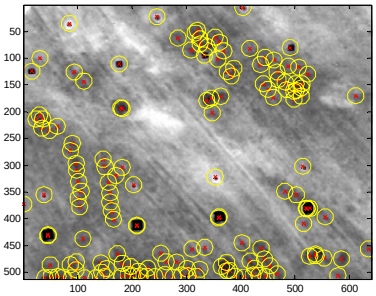

(b) Original MWIR with clusters.

Figure 2: Clusters obtained from the thresholded image.

As we can see from Figure 2, the ASOM clustering method gives many possible mine locations. We window out each putative mine location based on a standard deviation of pixels around the mine location. Figure 3 shows our windowing approach. In this figure, we start with a very small window, and increase the size of the window until the standard deviation of the pixels within each window starts increasing. The change in standard deviation is measured using the standard deviation of the current window and the past windows.

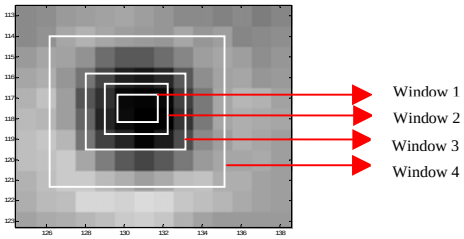

Figure 3: Windowing a potential mine.

In the figure we start with Window 1 and measure its standard deviation. Since most pixels in Window 1 are close in value, the standard deviation is small. Window 2 has a higher standard deviation than Window 1. Similarly Window 3 has a higher standard deviation than Window 2. Window 4 has the highest deviation of the four windows. The window size is increased until the rate of change in the standard deviation of at least 4 or 5 windows is close to a constant value. The window at which the change starts to become approximately constant is used to window the possible mine. Figure 4 shows the original image with all the putative mine location windowed.

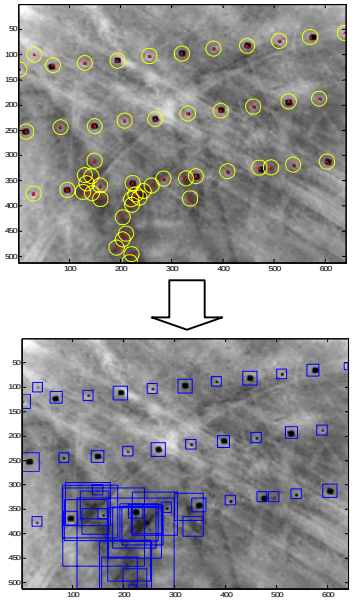

Figure 4: Output after applying the windowing technique.

3. CLUSTER INTENSITY VARIATION BASED BURIED MINE CLASSIFIER

To accurately classify buried mines using MWIR images, let's take a close look at their chips. Figure 5 shows four buried mine chips from night time MWIR images together with their histograms. It is clear that the pixel intensities of buried mine chips don't exhibit any particular common statistical distributions, which also implies that the traditional feature vector based classification schemes are less effective. This is largely due to the fact that it is difficult to construct the feature space with enough discrimination power.

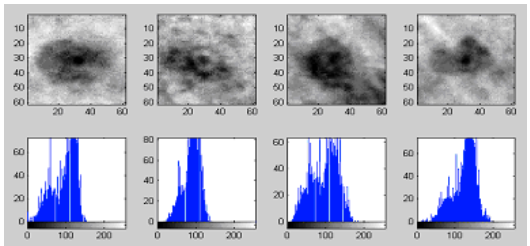

Figure 5: Buried mines in night time images and histograms.

Figure 6 shows four buried mine chips extracted from the daytime MWIR images. Compared with the night time chips shown in Figure 5, the daytime chips are lighter in intensity and pixel intensity changes are relatively small as well. Once again, it is clear that the buried mine chips from daytime images do not show any distinctive common features. Therefore, a new feature extraction approach is desired for both daytime and night time buried mine chips.

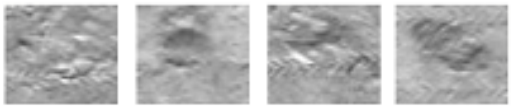

Figure 6: Buried mines from daytime MWIR images.

Our approach for the buried mine detection is to extract features based on the pixel intensity variations. Since the chip size is often too large (e.g., 50×50 pixels) to process in near real time, we apply our 3D unsupervised clustering method, *Adaptive Self-Organizing Maps* (ASOM), to extract the representative pixels from this patch. Compared to the traditional clustering methods, our ASOM does not need any prior knowledge of the cluster numbers. By self-learning, it finds the optimal number of clusters from the pixels of the image chip. Being able to estimate the number of clusters in an unknown image chip is significant since it is often impossible to have the knowledge of image chip content *a priori*. Unsupervised clustering method such as our 3D ASOM is essential in dealing with real world data processing, including the buried mines detection.

Our similarity-based 3D Adaptive Self-Organizing Map (ASOM) is used to find clusters in the windowed chips. For each pixel in the target chip, its location (x, y) and intensity value (z) form a vector $X(x, y, z)$ and is used for clustering. Instead of using the Euclidean distance between two vectors as a measure of dissimilarity, the Tanimoto distance is used to measure similarity between two vectors. It is defined as:

$$S(X, Y) = \frac{X^T Y}{\|X\|^2 + \|Y\|^2 - X^T Y} \qquad (3\text{-}1)$$

The clustering algorithm is similar to our ASOM clustering algorithm except that the above similarity instead of Euclidean distance is used as the measurement. It starts with one cluster, which is the first vector. The similarity between a new vector X and existing cluster nodes $Y_i (i = 1, \ldots, m)$ are first calculated according to equation (3-1). If the maximum value of $S(X, Y_i)$ is less than a predefined threshold value, which indicates the new vector is different from all the clusters, a new cluster is added. Otherwise, the winning node (the node with the largest similarity value) and its neighborhood nodes are updated.

After clustering, the intensity values of the cluster centers are lined up to form a vector *C*. The *N*-step (*N* = 6 in our system) difference of each vector is calculated as:

$$DC(k) = C(k + N) - C(k) \qquad (3\text{-}2)$$

The difference vector *DC* is used as a feature vector.

Once the clusters are estimated, we scan their pixel intensity values at the cluster centers row by row to form a feature vector. This concept is illustrated in Figure 7. The pixel intensity variations scanned from each row are concatenated to form one vector, called cluster variation feature (CVF) vector. There are some other scanning schemes including the vertical scanning and diagonal scanning. Different CVF vectors can be formed from different scanning schemes. In this paper, we mainly focus on the horizontal scanning.

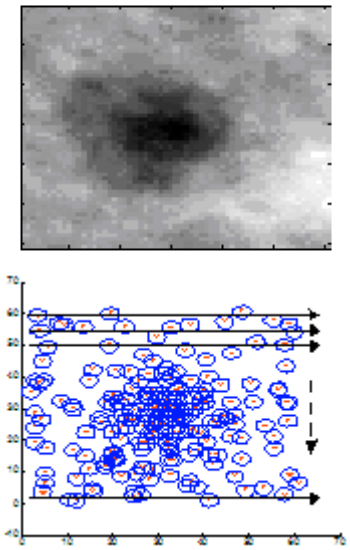

Figure 7: Buried mine image chip and clustering result.

Since the number of clusters in different chips is often different, the length of our buried mine cluster variation based feature vectors varies. Figure 8 shows four such feature vectors. These variable length features pose a formidable challenge to the traditional classifier design in which the feature vectors are *required* to have the same length. Therefore, a different classifier must be developed in order to use the CVF vectors to classify buried mines.

To visually compare CVF features, Figure 9 shows four CVF features associated with four clutter chips. An interesting observation is that the clutter CVFs are much shorter, which results from less number of clusters in the background clutter chips. By visually comparing the

CVFs of buried mines (Figure 8) and clutters (Figure 9), we can easily identify the differences, which implies that they can be used for the buried mines detection.

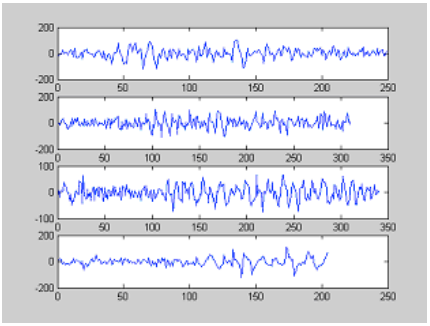

Figure 8: Feature vectors of four buried mines.

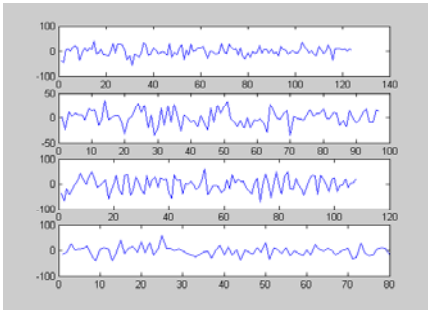

Figure 9: Feature vectors of four background clutters.

In order to perform classification using our variable length CVFs, *Kolmogorov-Smirnov* (KS) test has been used to compare the feature vectors extracted from each windowed target chip and each of the reference vectors in the signature library. The null hypothesis is that they have the same distribution. The test result for each target chip is 0, which means the hypothesis can be accepted. The test result for the background is 1, that is, the hypothesis must be rejected.

The Kolmogorov-Smirnov test (KS-test) tries to determine if two CVFs (with variable lengths) differ significantly. The KS-test has the advantage of making no assumption about the distribution of data, which means that it is nonparametric and distribution free. Let x_1, x_2, …, x_n denote an independent and identically distributed sample drawn from a population with unknown parameters θ_1, θ_2, …, θ_n. The KS-test statistic D_n is defined as

$$D_n = \sup_x |\hat{F}(x) - F_n(x)| \qquad (3\text{-}3)$$

where n is the sample size, $\hat{F}(x)$ is a fitted cdf, and $F_n(x)$ is the empirical cdf, a step function that increases by $1/n$ at each data value.

We can define the following detection ratio as:

$$T = \frac{Number\ \ of\ \ zeros\ \ of\ \ KS\ \ Test\ \ result}{Total\ \ Number\ \ of\ \ references} \qquad (3\text{-}4)$$

We can use the following majority-voting based detection rule: *If* $T \geq 2/3$, *the target chip is classified as a buried mine, otherwise it is classified as background clutter.*

Figure 10 shows the overall architecture of our buried mine detector. In this system, there are a number of buried mine signatures constructed off-line using the ground truth of MWIR images. We have found that different signatures are required in order to accurately detect the buried mines in daytime and night time.

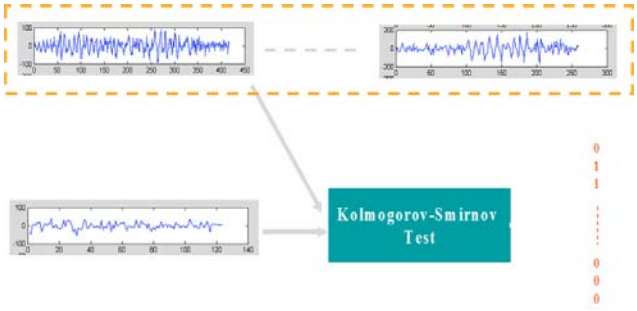

Figure 10: System architecture of buried mine classifier.

1. TESTING RESULTS USING REAL IMAGES

In order to demonstrate the buried mine detection process and verify the detection algorithms, we tested both daytime and night time images. This section shows the processsing and detection results. The results are compared with ground truth.

4.1 Daytime Test Results

A daytime image and its ground truth are shown in Figure 11.

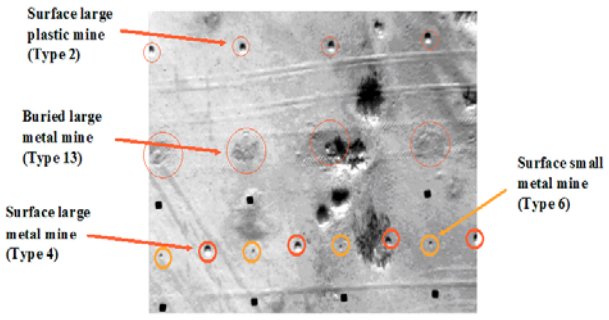

Figure 11: A daytime image and its ground truth.

Figure 12 shows the thresholded image, clusters based on wavelet thresholding and ASOM clustering method.

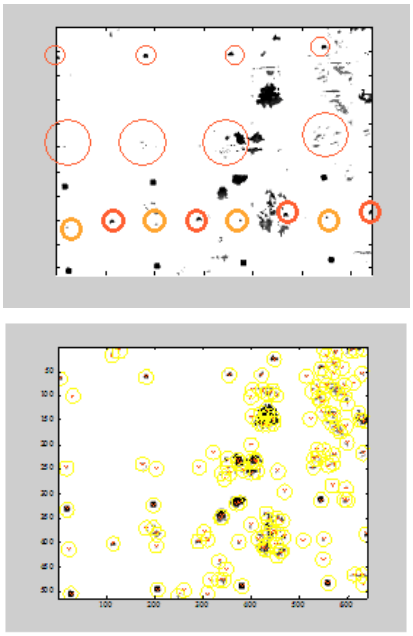

Figure 12: Thresholded image and ASOM clustering result based on the image given in Figure 11.

Figue 12 shows the library of 30 daytime buried mine chips. A corresponding 30 CVFs are constructed off-line and stored in the library for KS-test based buried mine detection.

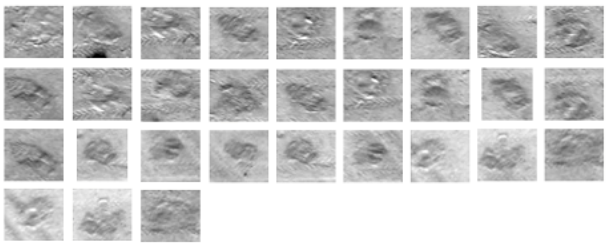

Figure 12:. A set of 30 daytime buried mine chips.

We then used our buried mine detection method to detect buried mines and the result is shown in Figure 13. The result indicates that 3 buried mines (type 13) are found, 1 missing and there is 1 false alarm. The missed buried mine is actually very hard to detect, even through visual inspection. If we carefully examine the image shown in Figure 11, it is clear that there are a number of bushes which appear to be buried mines. However, our algorithms have successfully discriminate them from the true buried mines. These results represent the effectiveness of our buried mine detector.

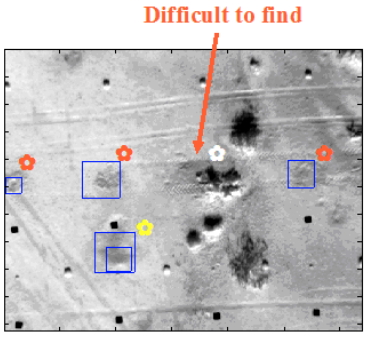

Figure 13: Daytime buried mine detection result.

4.2 Night Time Test Result

Figure 14 shows the night time image with the ground truth.

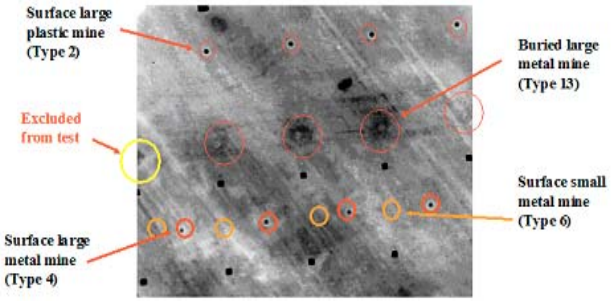

Figure 14: A night time image and ground truth.

Figure 15 shows the thresholded image and clusters based on wavelet transform and ASOM clustering method.

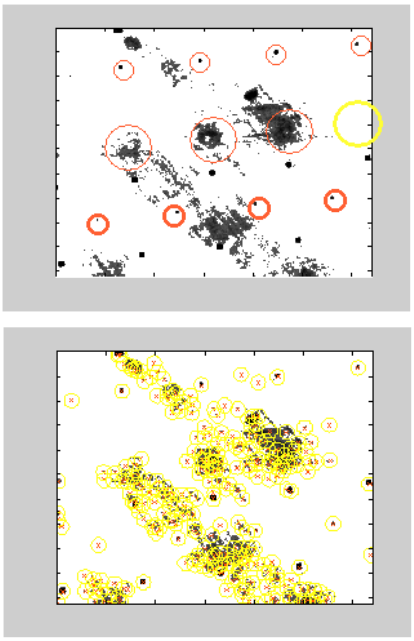

Figure 15: Thresholded image and ASOM clustering result based on the image given in Figure 14.

Figue 16 shows the library of 15 night time buried mine chips. A corresponding 15 CVFs are constructed off-line and stored in the library for KS-test based buried mine detection. Comparing to the daytime buried chips, these night time chips are darker and pixel intensity variations are more profound.

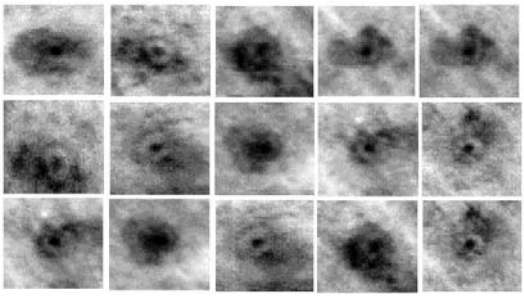

Figure 16:. The set of 15 night time buried mine chips.

The buried mine detection result is shown in Figure 17. The result indicates that 3 buried mines (type 13) are found, 1 mine is missing and there are 3 false alarms. The missing buried mine is extremely difficult even through the visual inspection.

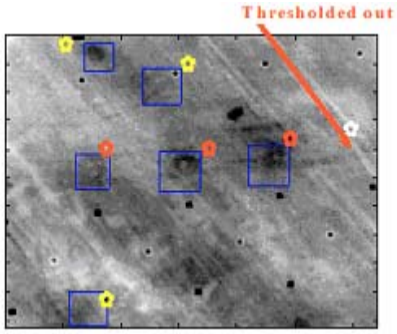

Figure 17: Night time buried mine detection result.

In addition to the test of MWIR images with known ground truth, we have also performed a blind test with various data sets in different environments, and the algorithms have performed well. These algorithms will be tested with multi-spectral data sets.

5. CONCLUSION

In this paper, we have described a nonparametric buried mine classifier using MWIR images. We start with our new image segmentation method based on the wavelet transform. In order to perform the statistical classification, we have applied Kolmogorov-Smirnov (KS) test. One major advantage of using KS test for buried mine detection is that we don't need to make any assumptions of the underlying statistical distributions associated with our cluster intensity variation profiles. We have conducted the extensive tests of our buried mine classifier using actual MWIR images taken during daytime and night time, and various background settings. The test results have shown that our nonparametric buried mine detection mechanism has a very good detection rate and low false alarm rate.

Acknowledgement: This work is supported by Army SBIR funding under contract W909MY-05-C-0011.

REFERENCES

♦ Barbour, B.A., Kordella, S., Dorsett, M.J., Kerstiens, B.L. (1996) "*Mine detection using a polarimetric IR sensor*", International Conference on the Detection of Abandoned Land Mines: A Humanitarian Imperative Seeking a Technical Solution, EUREL, pp. 78-82, 7-9 Oct. 1996.

♦ Batman, S., Goutsias, J. (2003) "*Unsupervised iterative detection of land mines in highly cluttered environments*", IEEE Transactions on Image Processing, Vol. 12, Issue: 5, pp. 509-523, May 2003.

♦ Beaven, S., Stocker, A.D., Winter, E.W. (2004) "*Joint multisensor exploitation for mine detection*", Proceedings of SPIE, Vol. #5415, April 2004.

♦ Behboodian, A., Scott, W.R., Jr., McClellan, J.H. (1999) "*Signal processing of elastic surface waves for localizing buried land mines*", 33rd Asilomar Conference on Signals, Systems, and Computers, vol. 2, pp. Pages:827 – 830, 24-27 Oct. 1999.

♦ Bowman, A.P., Winter, E.M., Stocker, A.D., Lucey, P.G. (1998), "*Hyperspectral infrared techniques for buried landmine detection*", Second International Conference on the Detection of Abandoned Land Mines, pp. 129-133, 12-14 Oct. 1998.

♦ Cheng, J., Miller, E. (2002) "*Model-based principal component techniques for detection of buried landmines in multiframe synthetic aperture radar images*", IEEE International Conference on Geoscience and Remote Sensing Symposium, Vol. 1, pp. 334 – 336, 24-28 June 2002

♦ Clark, G.A., Sengupta, S.K., Aimonetti, W.D., Roeske, F., Donetti, J.G. (2000) "*Multispectral image feature selection for land mine detection*", IEEE Transaction on Geoscience and Remote Sensing, Vol. 38, No. 1, January 2000.

♦ Filippidis, A., Jain, L.C., Martin, N.M. (1999), "*Using genetic algorithms and neural networks for surface land mine detection*", IEEE Transactions on Signal Processing, Vol. 47, Issue: 1, pp. 176-186, Jan. 1999.

♦ Filippidis, A., Jain, L.C., Martin, N. (2000) "*Multisensor data fusion for surface land-mine detection*", IEEE Transactions on Systems, Man and Cybernetics, Part C, Vol. 30, Issue: 1, pp. 145-150, Feb. 2000.

♦ Lundberg, M. (2001) "*Infrared land mine detection by parametric modeling*", IEEE International Conference on Acoustics, Speech, and Signal Processing, Vol. 5, pp. 3157-3160, 7-11 May 2001.

♦ Hu, Ming-Kuei, 1962, "*Visual Pattern Recognition by Moment Invariants*", IRE Transactions on Information Theory, February 1962, pp.179-187

♦ Svensson, L., Lundberg, M. (2001) "*Land mine detection in rotationally invariant noise fields*", Proceedings of the 11th IEEE Signal Processing Workshop on Statistical Signal Processing, pp. 170-173, 6-8 Aug. 2001.

♦ Svensson, L., Lundberg, M. (2002) "*Dual-band land mine detection using a Bayesian approach*", IEEE International Conference on Acoustics, Speech, and Signal Processing, Vol. 2, pp. 1297-1300, 2002.